

Unique Changes of Ganglion Cell Growth Cone Behavior Following Cell Adhesion Molecule Perturbations: A Time-Lapse Study of the Living Retina

Perry A. Brittis,¹ Vance Lemmon, Urs Rutishauser,* and Jerry Silver²

Department of Neurosciences, *Department of Genetics,
Case Western Reserve University, Cleveland, Ohio 44106

In the mammalian retina, multiple mechanisms are responsible for guiding retinal ganglion cell axons to the optic fissure. In the present study we have used time-lapse videomicroscopy to show that, within the center of the retinal neuroepithelium, growth cones use a scaffold of previously formed axons as a substrate for guidance. High magnification time-lapse videomicroscopy of normal growth cones in the midretina have shown that they have the ability to alter their shape from long, streamlined forms that hug other axons to more flattened forms that move between axons or neuroepithelial endfeet. In studies on the role of specific cell interactions in these events, Fab fragments against L1 and NCAM, administered either alone or in combination, were found to have dramatic and distinct effects on retinal ganglion cell growth cones. Anti-L1 Fab fragments severely disrupted radial growth cone orientation and rate of outgrowth. The anti-L1-treated growth cones initially stalled for 2 h, then changed direction and, thereafter, resumed an elongation rate twice as fast as in control preparations. By contrast, anti-NCAM Fab did not affect growth cone direction, but caused subsets of growth cones to speed up initially, then to dramatically increase in size, stall, and eventually halt. These results imply that L1 and NCAM play different roles in the promotion and direction of axon growth and, along with repulsive molecules and physical channels, provide es-

sential information for the unidirectional growth of retinal axons into the optic fissure.

INTRODUCTION

During developmental stages, ganglion cell axons from all radial positions within the cup-shaped retinal neuroepithelium unerringly navigate a trajectory that will bring them to a small opening in the posterior pole of the eye. This opening, known as the optic fissure, is the sole doorway that allows axons to exit the retina and join the optic nerve (Mann, 1969). The intraretinal projection is not built simultaneously but, rather, by a wavelike progression of axon initiation that begins at the optic fissure and ends at the retinal periphery (Goldberg and Coulombre, 1972; Halfter *et al.*, 1985). It has been suggested that one link in the chain of events that orchestrates this unique radiating sequence in embryonic rats involves the center-to-periphery regression of a proteoglycan-containing matrix that sweeps over the immature ganglion cells and may play a role in grossly constraining the path of their axons away from the retinal periphery (Snow *et al.*, 1991; Brittis *et al.*, 1992; Brittis and Silver, 1995). It is equally important to identify those positive outgrowth cues on the central side of the repulsive interface that help to promote growth of the retinal axons with such remarkable fidelity toward the optic fissure (Halfter and Fua, 1987).

The neuroepithelial cells that channelize the walls of the optic fissure could help lead pioneering fibers in the

To view and download the movies published in this paper, please visit the internet web site titled Neurons and Their Growth Cones at <http://gramercy.ios.com:80/~pab9/>

¹ Current address: Department of Experimental Pathology, UMDS, Guy's Hospital, London Bridge, London SE1 9RT, UK.

² To whom correspondence should be addressed at Department of Neurosciences, Case Western Reserve University, 10900 Euclid Ave., Cleveland, OH 44106-4975. Fax: (216) 368-4650.

proper direction toward their targets (Suburo *et al.*, 1979; Silver and Sidman, 1980; Krayanek and Goldberg, 1981; Brittis and Silver, 1995). However, for the overwhelming majority of axons that originate farther distally in the retina, the only substrata that are oriented in the direction of the fissure are the previously formed axons themselves. Thus, it is possible that growth-promoting axon-axon interactions, together with repulsive cues from the extracellular matrix, could play synchronous roles in generating the radial pattern of the intraretinal nerve fiber layer. A body of evidence, largely from studies of invertebrates, has convincingly shown the importance of fiber-fiber interactions mediated by specific adhesion molecules during formation of the complex network of nervous system tracts (Raper *et al.*, 1983; Bastiani *et al.*, 1985; Easter and Taylor, 1989; Chitnis and Kuwada, 1990; Wilson *et al.*, 1990). In vertebrate nervous systems, evidence that axons can guide other axons, either by positive (Lander, 1987; Landmesser *et al.*, 1988; Doherty and Walsh, 1989; Bixby and Jhabvala, 1990; Kim *et al.*, 1991) or negative influences (Kapfhammer and Raper, 1987; Godement *et al.*, 1990, 1994; Sretavan *et al.*, 1994), has also been presented. In the developing retina, axon deflection experiments have demonstrated that growth cones tend to faithfully reiterate the radiating trajectory of the resident axon scaffold even when growing in the wrong direction (Halfter and Deiss, 1986; Brittis and Silver, 1995). With regard to normal development, this observation not only reinforces the need for a repulsive force in the retinal periphery that would disallow the potential for wrong-way growth, but also suggests that, once growth cones are headed in the correct direction, growth-promoting interactions between retinal axons may constitute an essential means for guiding the contingent of follower axons out of the eye.

L1 (Lindner *et al.*, 1983; Moos *et al.*, 1988) and the neural cell adhesion molecule (NCAM) (Burskirk *et al.*, 1980; Cunningham *et al.*, 1987), both members of the immuno-

globulin gene superfamily, are abundantly expressed on axons. In addition, NCAM is often found in the glial environment (Silver and Rutishauser, 1984). *In vitro*, L1 and NCAM can promote retinal ganglion cell axon growth (Drazba and Lemmon, 1990). As these two CAMS have been localized to the early developing mammalian visual pathway, they are good candidates for mediating critical interactions during axonal growth and guidance (Silver and Rutishauser, 1984; Lemmon and McLoon, 1986; Hankin and Lagenaur, 1994). In this article we have used specific adhesion-blocking anti-L1 and anti-NCAM Fab's to investigate the potential role of L1 and NCAM in providing precise unidirectional radial signals for axon outgrowth in the intact mammalian retina.

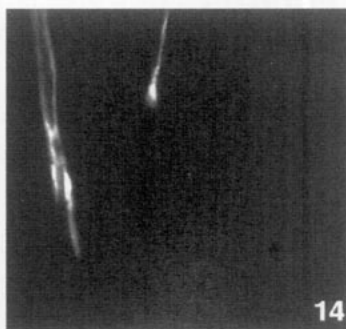
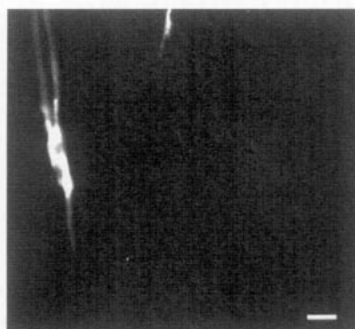
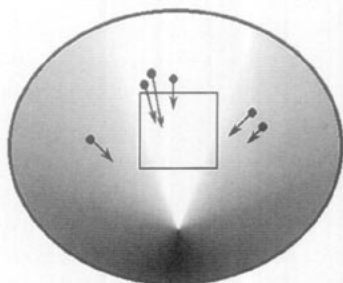
Immature retinal ganglion cells and their precursors, which span the entire retinal neuroepithelium, can be labeled with DiI from the ventricular endfoot surface in living rat retinal wholemounts without disrupting or contaminating the pial surface along which their axons grow. With the use of high resolution time-lapse videomicroscopy of living preparations, we were able to follow the course of normal ganglion cell axons as they elongate adjacent to the glial limitans within the center of the retina. Following the application of Fab's against L1 and NCAM, both separately and in combination, we have been able to document with time-lapse videomicroscopy various types of altered growth cone behaviors. We present evidence to show that, within the center of the retinal neuroepithelium, L1 and NCAM play simultaneous but different roles in directing and stimulating the forward progress of growth cones.

RESULTS

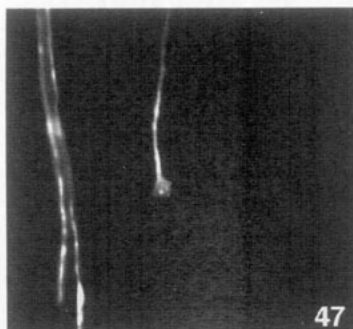
Normal Growth Cone Pathfinding within the Center of the Retina

In an effort to better understand the changes in axon growth caused by L1 and NCAM antibody perturba-

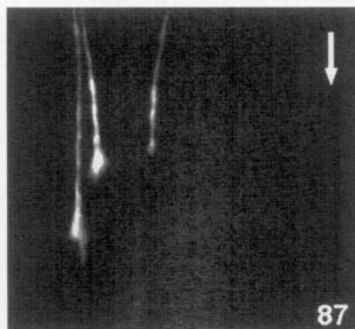
FIG. 1. Time-lapse sequence of normally growing retinal ganglion cell axons as they traverse the retinal neuroepithelium from the far retinal periphery to the optic fissure in E14.5 retinal wholemounts. (Cartoon) Schematic of a whole-mounted retina demonstrating the location of the DiI-labeled fibers at the time when the first frame was collected. The optic fissure is located at the bottom of the diagram (heavily shaded region). The box shows the camera area where the first frame was collected. Large arrows in the top right corners signify that the camera (i.e., boxed area) was moved in the indicated direction to continuously track the growth cones. Time elapsed from the first image in minutes is shown in the bottom right corners. The axons originated from cell bodies that were labeled from the ventricular surface of the peripheral neuroepithelium. All of the axons observed grew continuously, without any lengthy stops or retractions, with a linear trajectory toward the optic fissure. The growth cones consistently alternated between slim spadelike lamellipodial shapes, which lacked definitive filopodia (as seen at 47 and 105 min), and lamellipodial forms with short, forwardly directed, filopodial projections (as seen at 200 min, small arrow). There was little evidence of large movements across fascicle boundaries and, for the most part, the overall trajectories of individual axons were parallel. Oftentimes, axons grew on top of other axons that had preceded them (as seen at 231 min). As some of the growth cones approached the optic fissure they defasciculated (as seen at 285 and 326 min, small arrow). In this preparation nasal (arrowhead at 285 min), central, and temporal axons were labeled at the same time. All of the axons arrived at the optic fissure at the same time. As the growth cones approached the fissure they became larger and slowed down (as seen at 326–481 min, small arrows). The area of the optic fissure was marked by a fluorescent bead (arrowhead at 341 min). Scale bar represents 10 μ m.



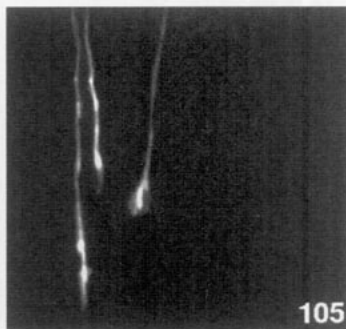
14



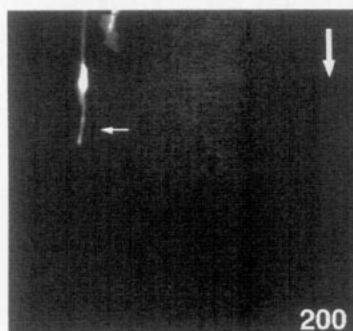
47



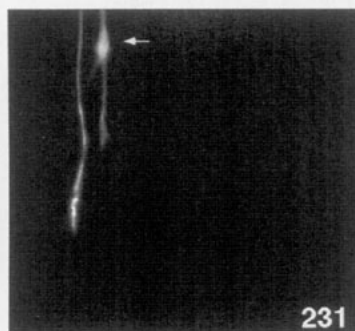
87



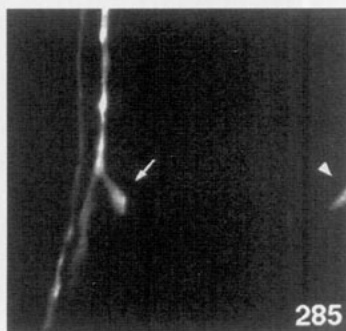
105



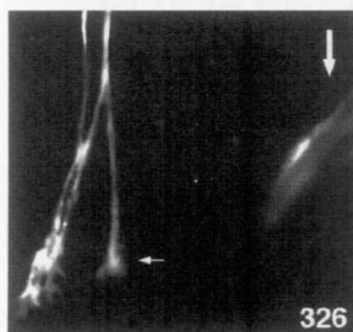
200



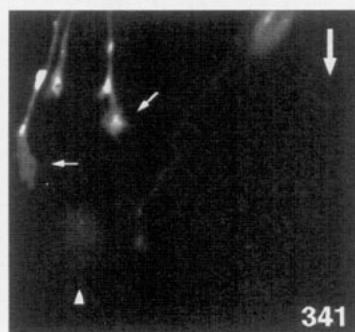
231



285



326



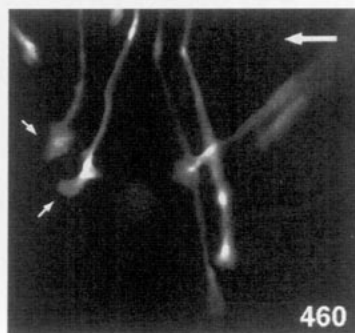
341



351



397



460



481

tions, we compared these effects with the results obtained from control preparations which were grown in media alone ($n = 30$ retinas), nonspecific goat anti-mouse IgG (500 $\mu\text{g}/\text{ml}$, $n = 25$ retinas), or anti-laminin Fab fragments (500 $\mu\text{g}/\text{ml}$, $n = 30$ retinas). Axons which were grown in media alone (Fig. 1) were tipped with small streamlined growth cones with an area of $51 \pm 21 \mu\text{m}^2$ (mean \pm SEM) (Fig. 7B). The rate of outgrowth of axons grown in media alone, goat anti-mouse IgG, or anti-laminin Fab's was 45 ± 9 , 48 ± 1 , and $51 \pm 8 \mu\text{m}/\text{h}$, respectively (mean \pm SEM) (Fig. 7A). There were no lengthy stops or retractions and all of the growth cones studied grew with pinpoint accuracy toward the optic fissure (Figs. 1 and 8A). As the growth cones traversed the middle of the retinal neuroepithelium they remained within the same focal plane near the pial surface. They consistently alternated between slim, spadelike lamellipodial shapes, which lacked definitive filopodia, and lamellipodial forms with short (no longer than $10 \mu\text{m}$) forwardly directed, filopodial projections (usually no more than two) (Figs. 1 and 8A). At these early stages, there was little evidence of large movements across fascicle boundaries and, for the most part, the overall trajectories of individual axons were parallel (Fig. 8A).

High Magnification of Growth Cone–Axon and Growth Cone–Growth Cone Interactions

Time-lapse imaging at high magnification revealed that retinal ganglion cell growth cones grew very close to previously established axons. When time-lapse movies ($n = 4$ movies) were viewed frame by frame there was

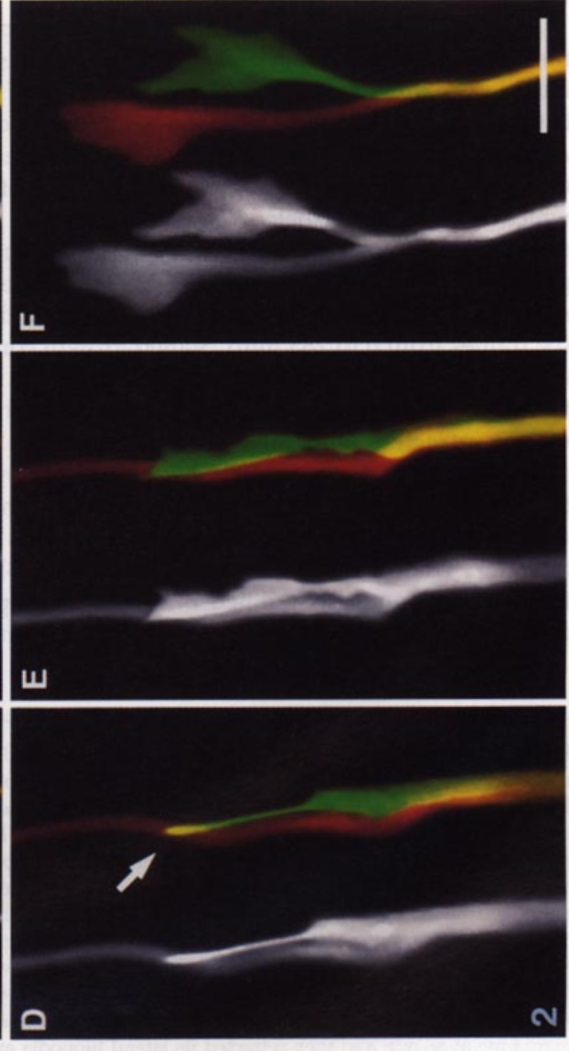
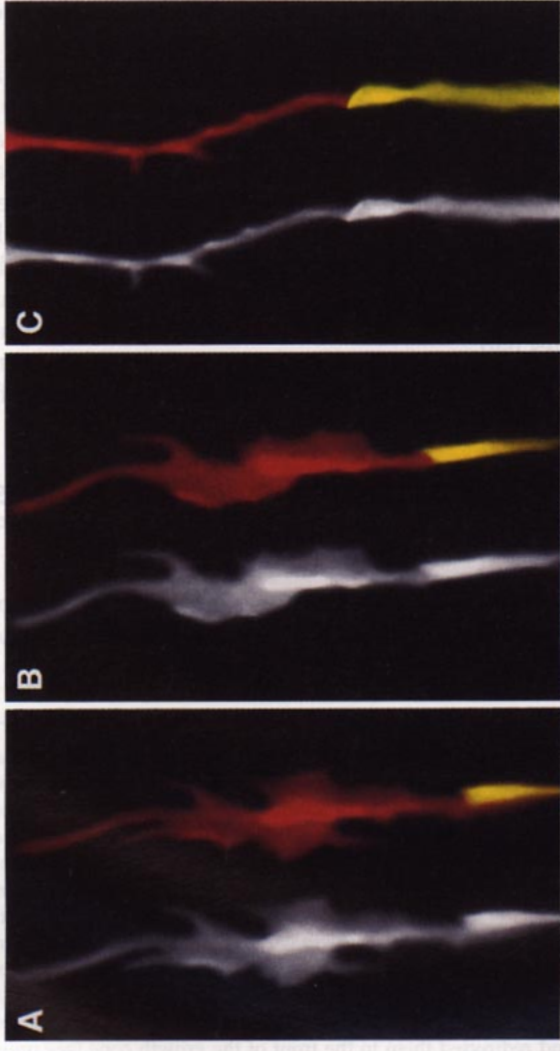
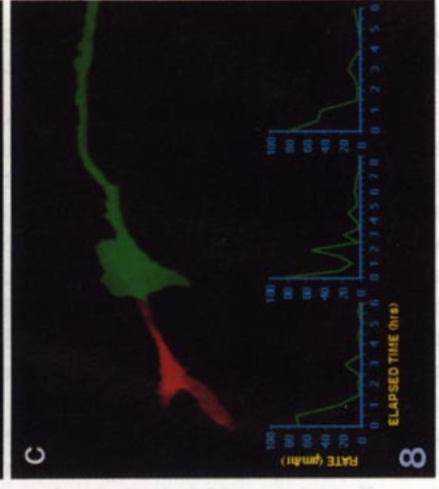
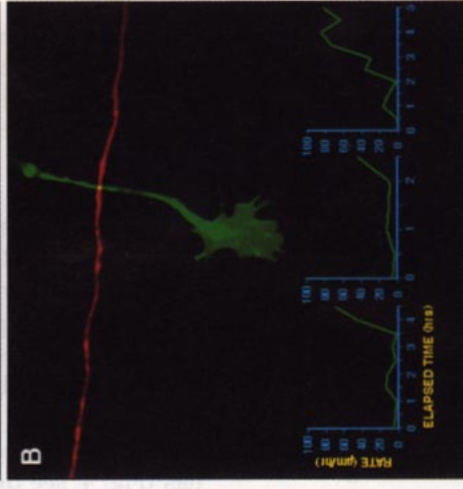
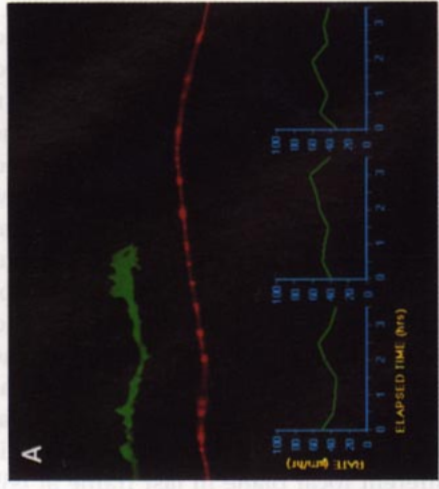
a repeating sequence of growth cone morphologies (Figs. 2A–2F). One type of growth cone morphology that was very difficult to detect, and not apparent at lower magnifications, was a flattened lamellipodial shape that contained no visible filopodia (Figs. 2A and 2B). It fit exactly to the contour of the labeled axon over which it grew and, in still frame, it appeared to be tightly associated. When viewed by time-lapse microscopy, such streamlined growth cones had the ability to project one visible fingerlike, filopodial projection which was approximately $10 \mu\text{m}$ long (Fig. 2D). As these filopodia projected straight ahead, the shaft of the filopodia showed little affinity for the other axon except for the tip which usually anchored itself to the axon with which it was associated (Fig. 2D). Sometimes the filopodium left the parent axon to move onto a close neighbor. In either case the filopodium then expanded into a larger streamlike veil (Fig. 2E). When growth cones such as these moved more laterally, the lamellipodia could become more pancake-shaped (Fig. 2F). Importantly, in every case examined, the proximal portion of the axon always stayed fixed to the parent axon. Two axons could elongate on each other in tandem. However, when this occurred, growth cones always stayed at least one growth-cone-length apart. If the trailing growth cone caught up with the other and made contact from behind, it remained active but ceased forward progress until the lead growth cone was well ahead (Fig. 2C). The follower growth cones that were observed never passed those ahead of them. This entire sequence of axon–axon interactions (Figs. 2A–2F) repeated itself as the growth cones made their way to the optic fissure.

FIG. 2. High-magnification time-lapse sequence of growth cone–axon interactions. Original black and white image is on the left side of the figure. Growth cones were manually separated and pseudocolored to better illustrate the different growth cone morphologies. (A and B) Growth cones (yellow–green) which were closely apposed to other axons (red) were streamlined in shape and almost undetectable. (C) The yellow–green growth cone began to lift off the red axon (D) and then extended one visible filopodia and made what appeared to be a small discrete contact with the red axon. (E) The lead filopodia then became more lamellipodial in shape and had more surface area. (F) The one-time, heavily fasciculated growth cone lifted its lamellipodia and shaft off the axon into a different focal plane (presumably onto the overlying endfeet). In (F), notice the relatively large space between the growth cone (along with its most distal axon portion) and the other axon. The distal axon remained fixed in position in tandem with the other axon (yellow area). In successive frames (not shown) the growth cone again became streamlined as shown in (A) and resumed growth along the same axon. These frames illustrate that growth cones can quickly alternate between substrates *in vivo*. Time between images equals about 10 min. Scale bar, $10 \mu\text{m}$.

FIG. 8. Graphs and images illustrating changes in growth cone rate, directionality, and morphology over time. Three representative growth cones representing each category, chosen from nine different retinal preparations, were tracked. The growth cones or axons which traversed the neuroepithelium first were falsely colored red, whereas newly arriving growth cones were colored green. (A) Changes in growth cone rate in control preparations. As the streamlined growth cones followed a linear trajectory toward the optic fissure their rate of outgrowth remained relatively constant. (B) Growth cones incubated in the presence of L1 Fab fragments were drastically perturbed. At first these growth cones were very active, became large and lamellipodial in shape, and traveled only small distances. After about 3 h the growth cones became more spadelike in shape and traversed the retinal neuroepithelium with increased rates at oblique angles. (C) At first, Fab fragment binding to NCAM caused the growth cones to increase their speeds. Over time, the perturbed growth cones became very large and lamellipodial in shape and decreased their rate of outgrowth. Perturbation did not affect axon guidance. Large growth cones were often seen growing on top of other axons which had a linear orientation.

...the experimental methods for the criteria used to select

...the criteria used to select



8

2

Anti-L1 Perturbation Causes Profound Changes in the Direction and Rate of Axon Outgrowth

To assess the degree to which L1 contributes to radial axon guidance in the midretina, presumptive retinal ganglion cell bodies in E14.0 living retinal wholemounts were labeled with Dil and incubated in the concentration of anti-L1 Fab's (500 $\mu\text{g}/\text{ml}$, $n = 25$ retinas) that best allowed for antibody tissue penetration (see also Experimental Methods). The effects of antibody perturbation on axon guidance were assayed within an area approximately 200 μm dorsal to the optic stalk (Figs. 3 and 7A, cartoon). Eighty percent of the 100 randomly selected growth cones incubated in the presence of anti-L1 Fab fragments displayed striking abnormalities (Figs. 3 and 4; see Experimental Methods for the criteria used to select the growth cones).

Anti-L1 incubation caused an obvious disruption of the usual pattern of axons in every retina that was examined. In the presence of anti-L1 Fab, the onset of perturbation took place within 3 h following antibody addition. At E14.5, the developmental stage of antibody treatment, there was a previously formed central core of axons which was also Dil labeled. The newly formed growth cones, which grew through the more mature central core, gradually became very large (Fig. 7B) and eventually stalled (Fig. 3, see frames from 0 to 119 min, and Fig. 4, see frames from 0 to 283 min). Stalled growth cones had a flattened lamellipodial shape (Fig. 8B) and were usually facing the optic fissure. The perturbed growth cones were very active and, thus, had the ability to extend and retract their lamellipodia. This type of growth cone behavior resulted in no net forward progress of the axon. Anti-L1-treated growth cones remained in this stalled transitory conformation for about 2 to 4 h (Fig. 8B) until they became more streamlined in shape, made perpendicular turns (Fig. 3, see frames from 126 to 150 min, and

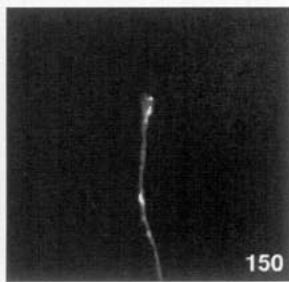
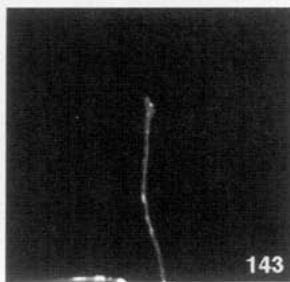
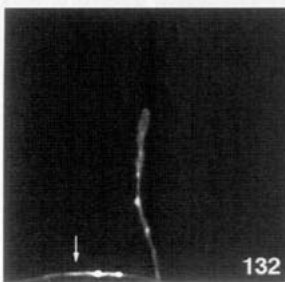
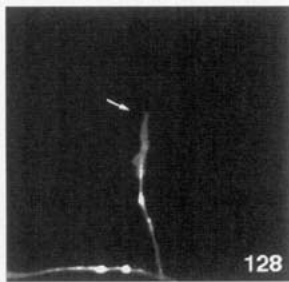
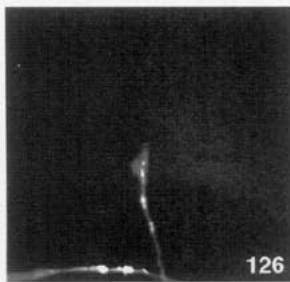
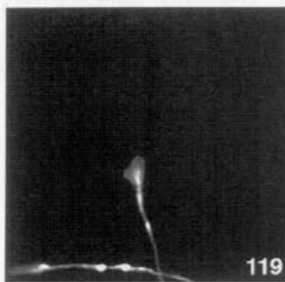
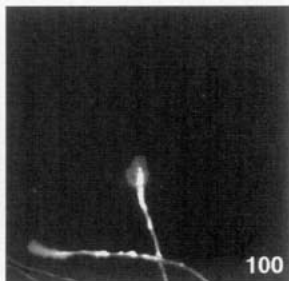
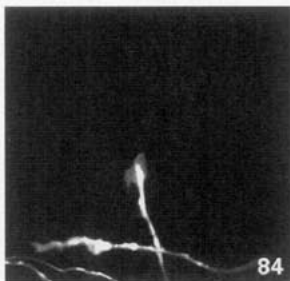
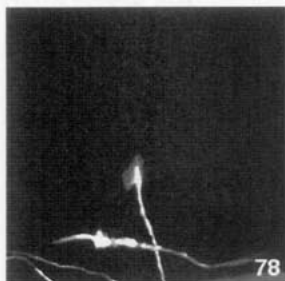
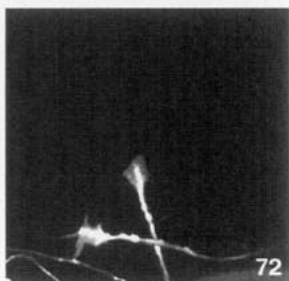
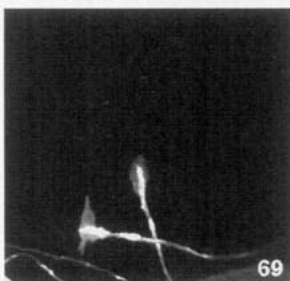
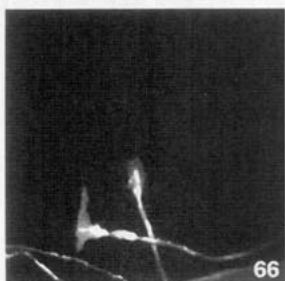
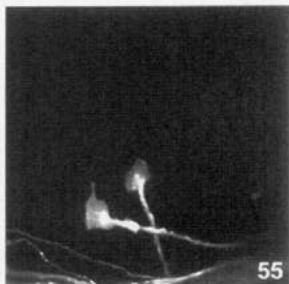
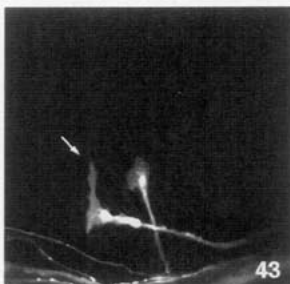
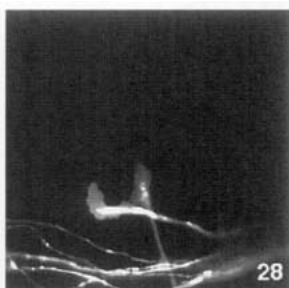
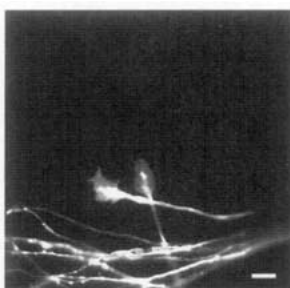
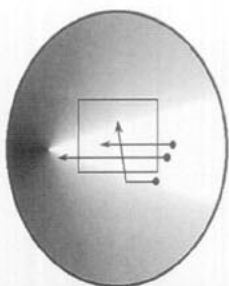
Fig. 4, see frames from 355 to 685 min) and increased their rate of migration (Fig. 8B). The aberrantly directed growth cones were either the same size or smaller than normal growth cones. They continued to traverse the neuroepithelium albeit at a faster-than-control rate and orthogonal to the previously formed central core of axons (Fig. 3, see frame at 128 min, and Fig. 4, see frames at 423, 438, 469, and 488 min, and Fig. 8B). A smaller population of axons made an abrupt 180° turn and grew toward the retinal periphery (Fig. 4, see frames at 355 and 400 min). As a result of this growth cone misrouting, the resultant nerve fiber layer became progressively disorganized (Fig. 4, see frame at 685 min). Although the initial fanlike pattern could still be distinguished in treated retinas (Fig. 4, see different focal plane in last frame at 685 min), many of the newly added axons formed a completely random network across the entire neuroepithelium.

In control preparations lacking anti-L1, the entire nerve fiber layer was always very stable and never shifted its position within the retinal neuroepithelium (Fig. 1). Conversely, the patterns of labeled axons established before antibody treatment appeared to slowly shift laterally after incubation in anti-L1 Fab (Fig. 3, note frame of reference does not change during the entire sequence). This slow movement was most unusual and was not simply the result of the entire specimen shifting because some reference growth cones remained stationary at a fixed point while other neighboring fascicles moved laterally.

Anti-NCAM Perturbation Causes Subsets of Growth Cones to Decrease their Rate of Outgrowth

Twenty-five living retinas were grown in the presence of anti-NCAM Fab fragments (500 $\mu\text{g}/\text{ml}$). Thirty per-

FIG. 3. Time-lapse sequence of two growth cones perturbed by anti-L1 Fab fragments. The first image was acquired 3 h after antibody treatment was begun. In this sequence of images the boxed area did not move during image acquisition. Growth cones incubated in the presence of anti-L1 Fab fragments displayed striking abnormalities. At E14.5, the developmental stage of antibody treatment, there was a previously formed central core of axons which were also Dil labeled (bottom of frames). Both the stalled growth cones (see first frame to 119 min) had a flattened lamellipodial shape. One was almost perpendicular to the other labeled fibers while the other remained parallel. The perturbed growth cones were very active but there was no net forward progress of the axon. Anti-L1-treated growth cones remained in this stalled transitory conformation until they became more streamlined in shape (see frames at 84 min and from 126 to 150 min) and increased their rate of migration. At this stage of the perturbation, many of the aberrant growth cones were either the same size or smaller normal growth cones. They continued to traverse the neuroepithelium albeit at a faster-than-control rate and orthogonal to the previously formed central core of axons. The other perturbed growth cone, which grew lateral to the more mature central core of Dil-labeled fibers, was very large but still followed the natural progression of axons. At 43 min, while still migrating, the growth cone projected a flat filopodium in the direction of the misrouted growth cone (arrow at 43 min). It repeated this one more time at 66 min and then retracted its lateral filopodia and redirected them to the front of the growth cone (see frames at 66, 69, 72, 78, and 84 min). Shortly thereafter, the growth cone became streamlined and continued to progress in a linear fashion toward the optic fissure. Notice how the pattern of labeled axons at the bottom of the frame, established before antibody treatment, appeared to slowly shift out of the field of view (move down the frame) throughout the entire movie. Scale bar represents 10 μm .



cent of the 63 randomly selected axons were affected by anti-NCAM incubation (Figs. 5 and 7). Perturbed growth cones were found within every anti-NCAM-treated retina. However, for rate analysis of our randomly selected sample, we only used those growth cones which could be traced for at least 60 min. It should also be stressed that the localized application of DiI only allowed us to visualize small axonal subpopulations within each retina. All of the anti-NCAM-perturbed growth cones were very different from those found in each of the control groups. At first, but only briefly, perturbed growth cones with streamlined morphologies moved faster than normal along other fibers (Fig. 8C). Shortly thereafter they became very sluggish (Figs. 7B and 8C) and gradually took on a lamellipodial shape with few visible filopodia (Fig. 8C). Initially, the lamellipodial veils did not spread out but were contained (Fig. 5, see frames from 0 to 134 min). Within hours, the growth cones grew larger than those found in either the control or the anti-L1 group (Fig. 7B) and became more pancake-shaped (Fig. 5, see frames from 181 to 494 min). It appeared as though the lamellipodial veils of affected growth cones were unable to make stable contacts with the substratum. At this stage of the perturbation, very few visible filopodia were extended even though the veils remained highly active. Thus, like those axons initially affected by the anti-L1 treatment, anti-NCAM Fab-treated growth cones remained motile but did not make any forward progress (Fig. 8C). Unlike the L1-treated axons, the anti-NCAM-treated axons never changed their direction of growth and always faced the optic fissure. These growth cones became larger and larger as they progressively filled with DiI-labeled membrane. In addition, it was not uncommon to see a pair of axons that were extending over each other (Fig. 8C) in which the leading growth cone began

to enlarge but neither its forward growth rate nor its linear trajectory were impeded (Fig. 5, see frames from 134 to 234 min). In turn, the fasciculating growth cone took on the aforementioned phenotypes and stopped (Fig. 8C). Once stalled, these perturbed growth cones did not leave the other axon (Fig. 5, see frames from 134 to 494 min). Lateral shifting of the nerve fiber layer was not observed in the anti-NCAM-treated preparations.

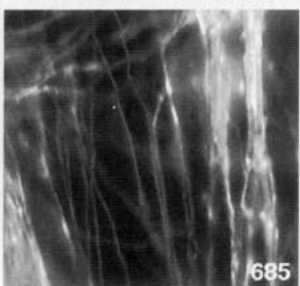
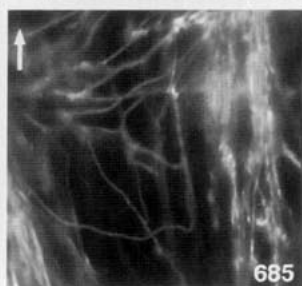
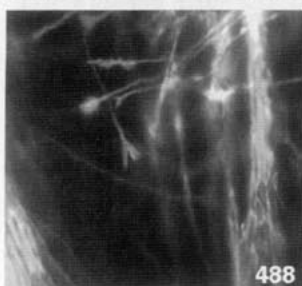
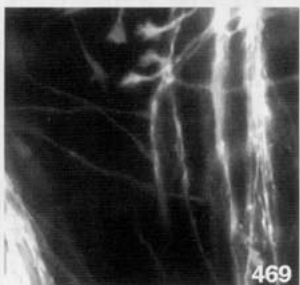
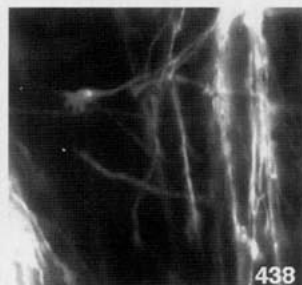
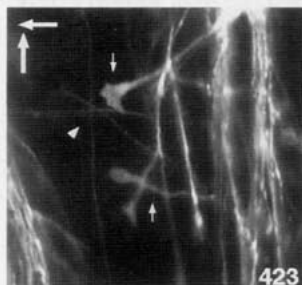
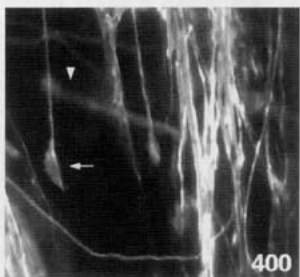
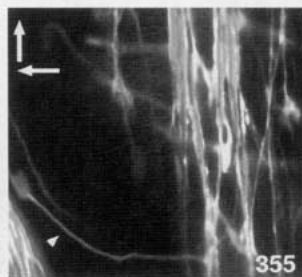
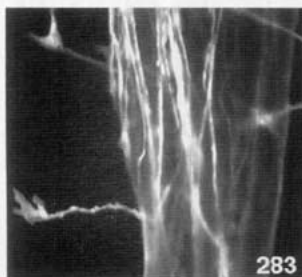
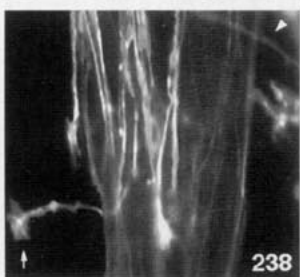
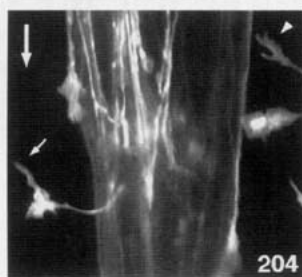
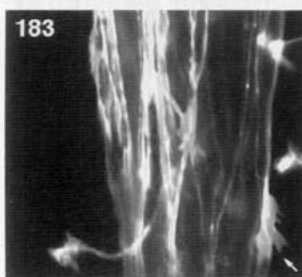
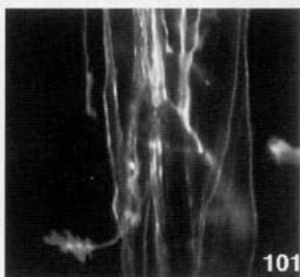
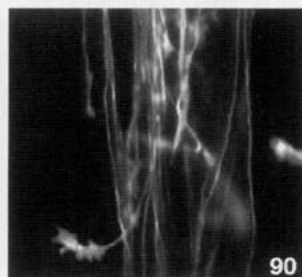
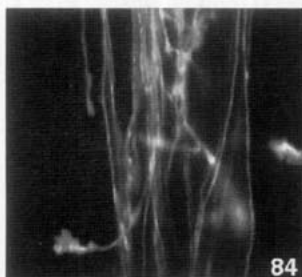
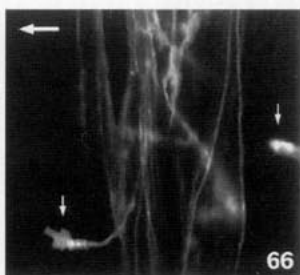
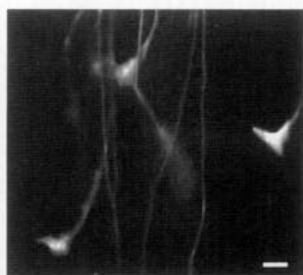
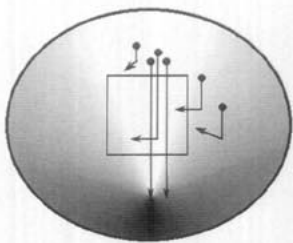
Anti-L1 and Anti-NCAM Administered Together

To learn whether or not axon growth could still occur when both CAMs were perturbed, retinal neuroepithelial preparations were incubated in both Fab preparations at the same time ($n = 5$ retinas). Although it was impossible to attribute the resultant perturbation to one or the other antibody, some general observations could be made. In each preparation the anti-L1-like effect predominated over the anti-NCAM-like effect on axon growth and guidance (Fig. 6). That is, most of the observed growth cones became large and eventually changed their orientation of outgrowth. Growth cones that did change direction did so with smoother, curving trajectories than occurred with anti-L1 alone. In addition, axons could be seen within the same field that remained idle and made no net forward progress during the duration of the experiment (Figs. 6B–6D). Interestingly, these axons were tipped with small growth cones which were lamellipodial in shape and lacked definitive filopodia. These lamellipodial forms were neither as large nor as active as those seen in the anti-NCAM-treated preparations.

DISCUSSION

By observing growth cone movements of fasciculating axons with high magnification time-lapse videomicros-

FIG. 4. Another time-lapse sequence of growth cones perturbed by anti-L1 Fab fragments. The first frame was collected 4 h after antibody addition. The boxed area moves as the camera follows the growth cones to the optic fissure. Growth cones incubated in the presence of anti-L1 Fab fragments displayed major changes in axon routing. At E14.5, the developmental stage of antibody treatment, there was a previously formed central core of axons which were also DiI labeled. Some of the newly formed growth cones maintained a linear trajectory toward the fissure as they grew over other fibers while passing through the camera field. However, even these axons could have very large growth cones (see small arrow at 183 and 400 min). The majority of the newly formed growth cones, which grew through the more mature central core, gradually became very large (small arrow at 66 min) and eventually stalled. Stalled growth cones had a flattened lamellipodial shape which remained very active and, thus, had the ability to extend and retract their lamellipodia (as marked by the small arrow at 204 min). This type of growth cone behavior resulted in no net forward progress of the axon. Anti-L1-treated growth cones remained in this stalled transitory conformation for about 2 to 4 h until they became more streamlined in shape, made perpendicular turns, and increased their rate of migration. At this stage of perturbation, many of the aberrant growth cones were either the same size or smaller than normal growth cones. They continued to traverse the neuroepithelium albeit at a faster-than-control rate and orthogonal to the previously formed central core of axons (small arrow at 66, arrowhead at 204, 238, 400, and arrow at 423 min, and notice the cohort of misguided fibers at 469 and 488 min). A smaller population of axons made an abrupt 180° turn and grew toward the retinal periphery (see growth cone marked by small arrow at 238 and follow it up to frame at 400 min; notice the axon marked by the arrowhead at 355 min). As a result of this growth cone misrouting, the nerve fiber layer became progressively disorganized (see final frame of sequence at 685 min). Although the initial fanlike pattern could still be distinguished in treated retinas, many of the newly added axons formed a completely random network of intersecting axons across the entire neuroepithelium (see different focal plane of last frame in third column at 685 min). Scale bar represents 10 μm .



copy, we have begun to appreciate the role of axon-axon interactions not only in the generation of fiber-bundling patterns but also in providing precise guidance information. Rapid, saltatorylike growth cone movements along other axons were typical of fasciculating fibers. This phenomenon was initiated by the protrusion of a single streamlined filopodium that tightly hugged the profile of the lead axon. This behavior was followed by expansion of the filopodium into a typical growth cone which could either project a single forwardly directed filopodium or leave the parent axon and move a short distance laterally. This "inchwormlike" behavior was repeated as the fasciculated growth cone moved along its neighbors.

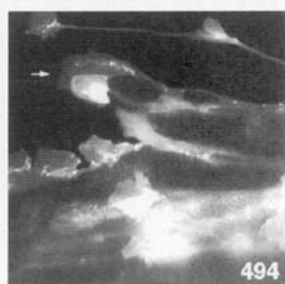
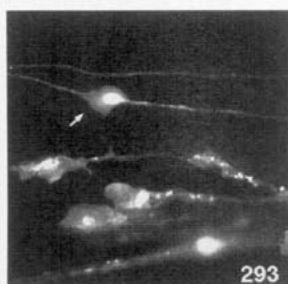
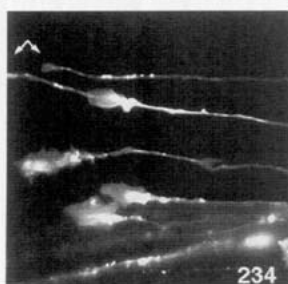
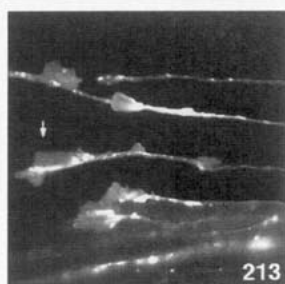
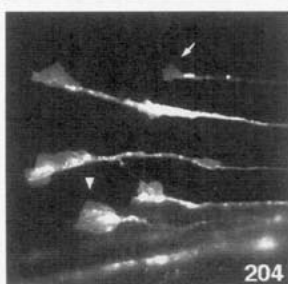
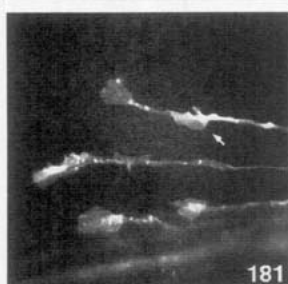
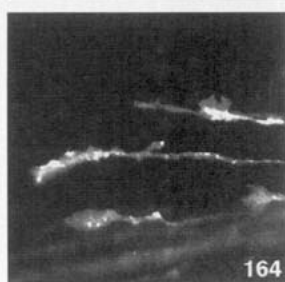
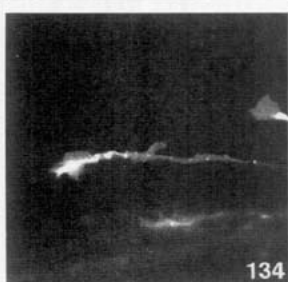
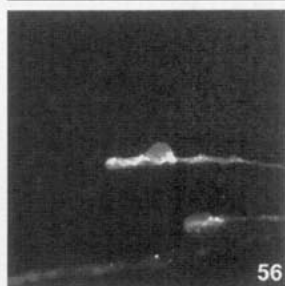
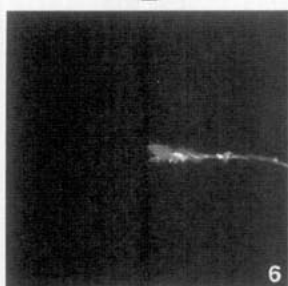
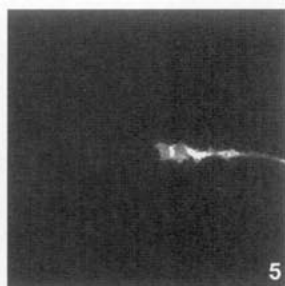
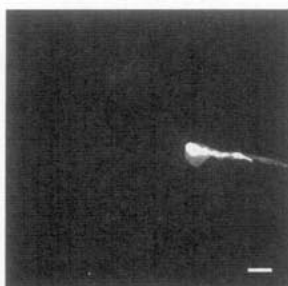
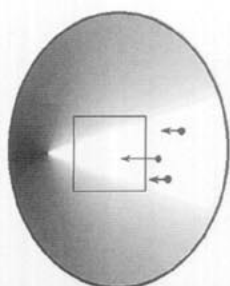
Molecules that mediate cell-cell interactions contribute to various aspects of growth cone behavior. The results presented here suggest that intraretinal ganglion cell axon growth and/or guidance can be severely altered by antibodies to L1 and NCAM, two abundant and well-characterized components of axons and the immature neuroepithelium. When either or both of these CAMs were perturbed by antibodies, growth cones within the midretina underwent a series of characteristic behaviors that revealed a change in substrate affinities. The consequences of these perturbations and substrate alterations led to both transient and long-lasting growth cone shape changes as well as pathway errors. Although perturbation was observed with both CAM antibodies, the type of alteration obtained was very different in each case. This suggests that L1 and NCAM appear to play distinct rather than redundant roles. Also the different effects of the two antibodies help to indicate that the possibility of steric hindrance, due to the antibody configuration on the surface of the axon, was not a key determinant in the altered growth behaviors.

Various experimental paradigms have shown that L1 can strongly promote neurite growth in culture (Lagenaur and Lemmon, 1987; Doherty and Walsh, 1989; Asou *et al.*, 1992; Lemmon *et al.*, 1992; Miura *et al.*, 1992; Hankin and Lagenaur, 1994), and antibodies to an L1-like mole-

cule in chicken have caused disruptions in axon pathfinding (Schlosshauer and Dutting, 1991). However, the ability of L1, or L1-like molecules, to guide precise rectilinear growth of one axon upon another, in addition to their role in fiber bundling (Stallcup and Beasley, 1985; Landmesser *et al.*, 1988), has not been extensively addressed. Our data suggest that L1 may function *in vivo* to direct filopodia tightly along other axons by focusing cytoskeletal components in order to ensure linear growth cone routing. Various investigators have shown that L1 can be positioned at points of axon-axon (Kobayashi *et al.*, 1992; Brittis and Silver, 1995) or axon-glia contact (Martini *et al.*, 1994) and have speculated that these "hot-spots" may serve to stabilize and reinforce points of growth cone adhesion (also see Smith, 1994). The notion that L1 may, in part, serve to stabilize or constrain retinal axon growth along a straight line, parallel to other axons, is supported by our observations that perturbation of L1 not only results in a meandering fiber pattern but also eventually increases the rate of axon outgrowth.

After treatment with L1 antibody, ectopic growth cones were more expanded and no longer traversed the neuroepithelium by projecting a single, slender filopodium. It is possible that perturbation of this particular CAM unmasked an innate tendency of the growth cone to turn or, alternatively, that turns may be stimulated by other substrate elements located on or between the neuroepithelial endfeet. Experiments designed by Overton (1979) have shown that growth cones are able to "perceive" physical contours with which they make frequent contact. In these studies when cultured growth cones were confronted with aligned collagen lattices in whole-mounted basal laminae they usually grew perpendicular to them. Perhaps anti-L1 made axon surfaces molecularly unrecognizable to growth cones thereby unlocking such a physical tendency to grow in a nonaligned fashion among the retinal ganglion cells. It is also possible that in the absence of L1 function, other molecules, such as cadherins, integrins (Reichardt *et al.*, 1989; Radies and Takeichi, 1993), or other Ig-class receptors,

FIG. 5. Anti-NCAM preparation. The first frame was collected 4 h after antibody addition. In this sequence of images the boxed area did not move during image acquisition. All anti-NCAM-perturbed growth cones were very different from those found in the anti-L1 and control groups. At first, perturbed growth cones with streamlined morphologies briefly moved faster than normal along other fibers (see frames from the start to 56 min). They then became very sluggish and gradually took on a lamellipodial shape with few visible filopodia (small arrow at 37 min). Initially, the lamellipodial veils did not spread out but were contained (see frames from 0 to 134 min). Within hours, the growth cones became more pancake-shaped (see frames from 181 to 494 min). At this stage of the perturbation, very few visible filopodia were extended even though the veils remained highly active. The anti-NCAM-treated axons never changed their direction of growth and always faced the optic fissure. These growth cones became larger and larger as they progressively filled with Dil-labeled membrane (large growth cones from 318 to 494 min). Some perturbed growth cones began to enlarge but neither their forward growth rate nor their linear trajectory were impeded (see frames from 134 to 234 min). The growth cones fasciculating on these axons also became large but eventually slowed down (small arrow at 181 min). Once stalled, these perturbed growth cones did not leave the other axon (see frames from 134 to 494 min). Notice the unperturbed streamlined growth cone (small arrow at 204 min) that passed through the same area where other larger growth cones traversed (from 204 to 234 min; compare the growth cone and axon marked by small forked arrow). Scale bar represents 10 μm .



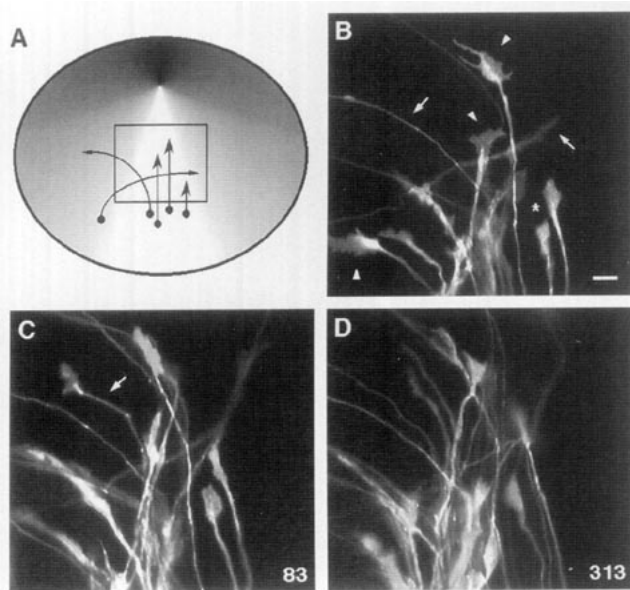


FIG. 6. Time-lapse sequence of growth cones incubated in both anti-L1 and anti-NCAM. (A) Schematic of a whole-mounted retina demonstrating the location of the DiI-labeled fibers at the time when the first frame was collected. In this sequence of images the boxed area did not move during image acquisition and the boxed region shows the camera area where the frames were collected. The anti-L1-like effect predominated over the anti-NCAM-like effect on axon growth and guidance. Most of the observed growth cones became large (arrowheads in B) and eventually changed their orientation of outgrowth (arrow in C). Growth cones that did change direction did so with smooth, curving trajectories (small arrows in B and C). Notice the axons that grew orthogonal to the other axons (small arrows in B). Some growth cones, though still active, remained idle and made no net forward progress during the duration of the experiment (marked by star in B and apparent in C and D). These axons were tipped with small growth cones which were lamellipodial in shape and lacked definitive filopodia. Scale bar represents 10 μm .

assumed priority in promoting neurite growth, albeit sinusously and in a haphazard direction. Alternatively, anti-L1 antibodies might have generated signals that lead to alterations in the function of other substrate recognition systems (Doherty and Walsh, 1992). Earlier work on retinal ganglion cells has shown that anti-L1 antibodies alter fasciculation in a manner most easily explained by disruption of multiple CAM functions (Cervello et al., 1991) rather than alterations in the expression of CAM levels. As the function of integrins and cadherins can be modulated by second messenger systems, it is plausible that they might mediate the renewed advance of growth cones in the presence of anti-L1 antibodies.

Many of the L1-affected growth cones were very active for about 4 h without gaining any forward progress. This type of stalling phenomenon has also been seen in *in vitro* experiments which have shown that when approached

from a non-L1 substrate, growth cone contact with a border of L1 usually caused a pause or collapse of the growth cone followed by renewed growth over the border (Burden-Gulley et al., 1995). *In vivo*, the transient nature of the arrest, followed by resumed growth in the presence of L1 antibodies, could be explained in several ways. One explanation of the stalling phenomenon could be that Fab incubation restricts L1-L1 homophilic interactions which then triggers an upregulation of other receptors capable of supporting renewed outgrowth. The 4-h growth cone stalling period might be sufficient time to reinsert new receptors at the growth cone surface. Such an upregulation of an alternative growth-supporting receptor, namely integrin $\delta 3$, has been observed in axons in response to a step gradient of a growth inhibitory proteoglycan in combination with laminin (Condic et al., 1993). The highest step achieved by growth cones can have a concentration of inhibitory chondroitin sulfate proteoglycan (CSPG) that would have repelled laminin-dependent neurite outgrowth had the initial step onto this surface been more steep (Snow and Letourneau, 1992). This type of receptor upregulation response could allow growth cones to utilize laminin more efficiently. However, the response for such a mechanism would likely occur more slowly than might have occurred if there had been receptor modification via a signal-cascade-induced phosphorylation event. Receptor upregulation may also play an important role in normal pathfinding when substrates change in different topographical locations and where growth cones stall for relatively long periods of time, such as at the entrance to the optic fissure (see Fig. 1) or at the pelvic girdle during peripheral nerve development (Tosney and Oakley, 1990). Another possible way to account for transient growth cone arrest is that anti-L1 antibodies, in addition to disrupting cell adhesion, also alter levels of intracellular second messengers that could affect growth cone or neural behaviors at the cytoskeletal level. There is evidence that anti-L1 antibodies alter intracellular Ca^{2+} levels (Schuch et al., 1989; Vonbohlen et al., 1992) and can alter phosphorylation patterns of growth cone cytoskeletal components (Atashi et al., 1992; Schachner and Maness, 1992). Taken together these experiments indicate that antibody binding to L1 or L1-L1 binding itself can generate signals that might transiently stop or start growth cone movements. A final possibility we do not favor is that there is a decrease in the efficiency of the antibody with time. Different growth cones continued to stop and restart throughout the entire experiment, suggesting that sufficient antibody titers were always present. Moreover, the antibodies were used at relatively high concentrations and for durations shorter than those used in other experiments where the antibodies had prolonged effects (Drazba and Lemmon, 1990; Smith et al., 1990; Barami et al., 1994).

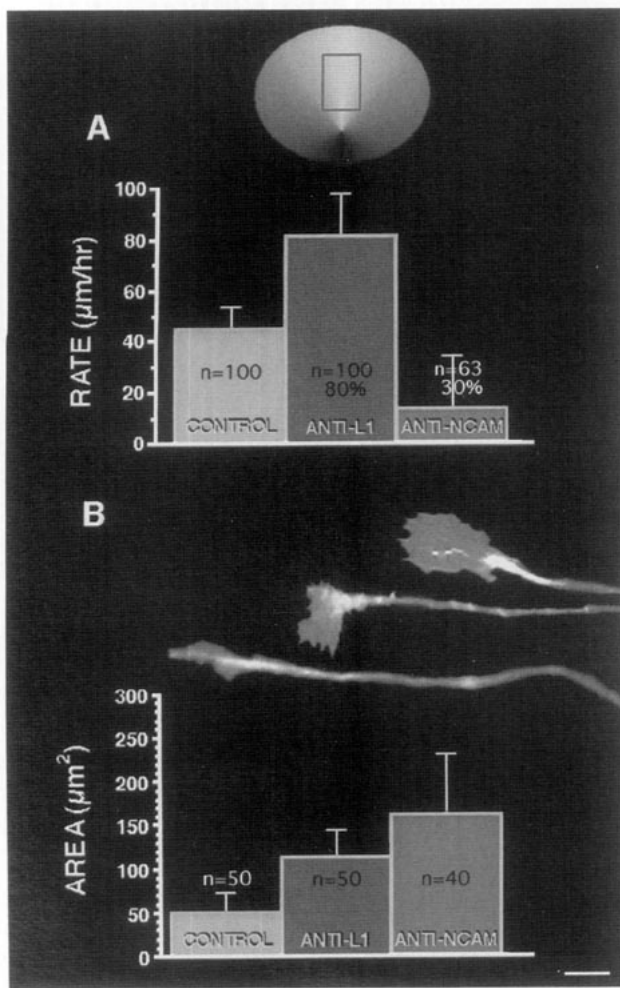


FIG. 7. Graphs illustrating average growth cone rates and area. See Experimental Methods for the criteria used to select the growth cones. (A) Average growth cone rate (mean S.E.M.), the number (*n*) of growth cones sampled, and the percent affected in the absence of antibodies or in the presence of either anti-L1 or anti-NCAM function blocking Fab fragments as they traversed the center of the retinal neuroepithelium over approximately 200 µm (as marked by red box in schematic). The control rate of outgrowth of axons grown in goat anti-mouse IgG, or anti-laminin Fab was 48 ± 11 µm/hr, and 51 ± 8 µm/hr (mean ± S.E.M.), respectively. (B) Average growth cone area (mean S.E.M.) in the absence of antibodies or in the presence of either anti-L1 or anti-NCAM during the growth cone stalling phase. A model growth cone for each corresponding category is above each column. Scale bar represents 10 µm.

NCAM Perturbation

Although studies have shown that anti-NCAM can alter the retinal projection at the optic fissure (Silver and Rutishauser, 1984), the intraretinal fiber pattern has most often been reported not to change significantly in the presence of anti-NCAM antibodies (Silver and Rutishauser, 1984; Rutishauser *et al.*, 1985; Halfter and Fua,

1987; Thanos and Bonhoeffer, 1987). These and our present studies in the rat were not able to detect gross changes in fasciculation that have been reported to occur in chick retinal flatmounts after antibody perturbation of the hinge region of NCAM (Pollerberg *et al.*, 1986). However, in the present time-lapse study, because of our ability to record even the most subtle changes in individual growth cone shapes and speeds, it was possible at high magnification to document changes in small subsets of axons that were not readily discernable in previous experiments.

Anti-NCAM-affected growth cones first increased their rates of outgrowth, then became sluggish and eventually stopped. Interestingly, the maximal rate of axon growth after anti-NCAM treatment was similar to that obtained after anti-L1 perturbation although the time courses of the effects were very different. This common effect may suggest that antibody disruptions by anti-NCAM and anti-L1 were able to induce a similar second messenger cascade, such as that described by Williams *et al.* (1994), that leads to a maximal rate of axon extension.

Both anti-L1- and anti-NCAM-treated axons contained very motile growth cones. However, unlike those treated with anti-L1, lamellipodia of NCAM-perturbed growth cones neither returned to a streamlined shape nor resumed production of obvious filopodia. Because growth cones perturbed by anti-NCAM did not "recover" their mobility, it would appear that effects of the antibody are dominant over other outgrowth-promoting molecules present in the retinal anlage.

The question remains as to why only a small subset of growth cones was affected by anti-NCAM treatment. One possibility is that there is only a narrow time window in which growth cones are most susceptible to anti-NCAM. While the surfaces of intraretinal endfeet do not express L1, they are highly NCAM immunoreactive. Thus, one of the functions of NCAM on axons may be to help promote axon-endfoot associations (Silver and Rutishauser, 1984). If, as previous studies suggest (Rager and von Oeynhausen, 1979; Silver and Sidman, 1980; Easter and Taylor, 1989; Williams *et al.*, 1991), growth cones receive information from both the endfeet surfaces and from other axons simultaneously, it may only be possible to interrupt axons with anti-NCAM at the precise time that the growth cone is solely dependant upon the endfoot for its growth-promoting information. It is interesting that although this is a rare event for fasciculating axons, the inhibition of NCAM at this precise time apparently leaves the growth cone stalled at the glial limitans.

Recent studies suggest that NCAM-mediated axonal growth depends less upon adhesion per se than it does upon the activation of a second messenger pathway that

results in calcium entry into neurons (Doherty and Walsh, 1994). Although the mechanism for the NCAM-induced halt of axons is unknown, it is conceivable that the internal pathways responsible for controlling forward progression could become improperly stimulated in some cells, thereby leading to a decrease in axon extension. Thus, the lamellipodial "motor" may remain active while not allowing for elongation of the axon. This type of growth cone behavior also supports the idea that independent mechanisms exist which control for axon extension and growth cone motility (Goldberg and Burmeister, 1986).

Anti-L1 and Anti-NCAM Combination

The antibody combination experiments show that neither L1 nor NCAM are absolutely required for growth of intraretinal axons. When incubated in both antisera, the majority of axons still elongated, albeit in a nondirectional fashion. Previous experiments have shown that, when forced onto the ventricular surface of the retina (a substrate never encountered by normal growth cones) ganglion cell axons grow randomly for long distances (Halfter, 1988; Brittis and Silver, 1994). Thus, retinal ganglion cell growth cones *in vivo* appear to be quite plastic in their ability to use multiple substrate cues for axon growth. The most obvious morphological change in axon growth, which differed from the addition of either anti-L1 or anti-NCAM alone, was that axons turned off course with curving rather than sharp angles. Thus, when NCAM and L1 function is blocked, other factors remain that can influence axon patterning. Altogether, these results imply that, while there might be redundancy in the substrate requirements that are generally growth permissive, there is a wide variety and specificity in the effects that individual molecules have on growth cone shape and precise fiber patterning (Payne et al., 1992; Goodman, 1994).

Finally, our results indicating that L1 plays a more conspicuous role in axon guidance compared to NCAM are consistent with studies using naturally occurring and induced genetic mutations. Although NCAM knockouts produce alterations in cell migration during brain development, massive disruptions in axon fiber pathways are not found (Tomasiewicz et al., 1993; Cremer et al., 1994). In marked contrast, human families with mutations in the L1 gene have gross structural abnormalities in major axon pathways such as agenesis of the corpus callosum and absence of the corticospinal tract (Rosenthal et al., 1992; Jouet et al., 1993, 1994; Van Camp et al., 1993; Vits et al., 1994). The fact that several different mutations in the L1 cytoplasmic domain cause gross brain malformations strongly implies that alterations in intracellular pro-

cesses or signals have occurred. Understanding how gene mutations and antibody perturbations disrupt CAM-mediated axon guidance will continue to be an important subject of future research.

EXPERIMENTAL METHODS

Animals

Timed pregnant Sprague-Dawley rats were obtained from a commercial vendor (Zivic-Miller, Pittsburgh, PA).

Preparation for Videomicroscopy

Embryos delivered by cesarean section at E14.0 were placed in ice-cold DMEM F-12. Eyes were removed with the aid of a dissection microscope using bright-field optics. The optic stalk was not disrupted and an approximate 100- μ m stump of nerve was left attached to the eyes when they were severed from the optic nerve. The eyes were then transferred to ice-cold calcium/magnesium-free medium and further dissected. The lens and the vitreous body were removed. The sclera and extraocular muscles along with the pigmented epithelium were also removed. The retinas were then gently whole mounted (vitreous surface facing up) onto black filter paper (Satorious). A total of 750 retinas were used for this study.

To timelapse retinal ganglion cells prior to and during axonogenesis, clusters containing 2 to 10 retinal ganglion cell bodies were labeled with the fluorescent dye DiI (Molecular Probes). It has been previously shown that young rat retinal ganglion cells retain a radial configuration while maintaining both vitreal and ventricular end-feet attachments to the retinal neuroepithelium (Brittis et al., 1992, 1995; Brittis and Silver, 1995). Thus, to avoid damaging the nerve fiber layer, ganglion cell labeling was achieved by manually coating finely ground DiI powder on top of the Satorius filters before whole mounting the retinas. An alternative and equally effective method was also used. DiI previously dissolved in DMSO was mixed into silicone grease. A microneedle was then used to apply the DiI/grease mixture to the ventricular side of the neuroepithelium. Immediately following the application of DiI, the embryonic preparations were maintained for 3 h with or without either anti-L1 (500 μ g/ml) or anti-NCAM (500 μ g/ml) antibody Fab fragments in 24-well clusters in DMEM F-12 culture medium supplemented with 10% fetal calf serum in a 5% CO₂ atmosphere at 37°C to allow for antibody penetration and for DiI to label the ganglion cell bodies, axons,

and growth cones. DiI-labeled preparations were then washed, placed in the appropriate antibody solution for the entire duration of the experiment, and then used for fluorescent imaging of the ganglion cells either prior to axon propagation or shortly thereafter.

Time-Lapse Imaging of Retinal Ganglion Axon Pathfinding

A Zeiss 405 inverted fluorescence microscope equipped with a heated air chamber was used to view the labeled retinal preparations. The retinal neuroepithelium was viewed with a 100 \times oil objective. Images were collected with an intensified CCD camera (Hamamatsu). Because of large light intensity differences, cell bodies and axons could not be imaged together in the same frame. Photodamage to living tissue was minimized by using neutral density filters and shutters placed in the light path. To rule out photodamage effects, antibody and fissure perturbations were also carried out in the absence of fluorescent light and checked manually every 3 h. Minor processes were sensitive to even the lowest light levels which greatly complicated our ability to study them. Time-lapse images were obtained using a UIC Image 1 system. Low light level fluorescence images were averaged (16–32 \times) and then stored on an optical disk recorder (Panasonic). Images were obtained at 1-min intervals (unless otherwise noted). Individual growth cones remained healthy under these conditions and were monitored for up to 12 h. Images were rigorously checked for correct focal planes every 2 to 5 min throughout the entire 12-h duration. Some images were acquired twice in two different focal planes with the highest possible neutral density filter in place. These images were later merged (summed) during image analysis for greater resolution.

Image Analysis

Journals within the Image 1 system were constructed to measure growth cone rate and area.

Criteria used to select growth cones for study/criteria used to study perturbed growth cones. All DiI-labeled growth cones studied were initially selected randomly and those that could be traced for more than 60 min were selected for further analysis.

Growth cone rate. The distance traveled by growth cone tips was measured every 10 frames (every 10 min) and summated.

Criteria used to define perturbed growth cones. (1) Aberrant rate of forward progress for more than 10 min, (2) marked directional changes in such a manner that

axons grew away from the optic fissure, or (3) a dramatic change in shape of the growth cone.

Growth cone area. Pixels that made up the growth cones found in both control and experimental conditions were thresholded. Individual thresholded growth cones were selected and measured by stamping a premeasured circle up to, and including, their base (stalk).

Pseudocoloring of growth cones. Growth cone sequences were repeatedly viewed with the Image 1 system and, in the appropriate still frames, boundaries of growth cone/axon borders were carefully traced. Each axon and growth cone was falsely colored pixel by pixel to assure the most accurate color separation.

Control and Experimental Antibody Production and Fab Generation

The rabbit polyclonal antibody to L1 used in these experiments was made by purifying rat L1 from P7 rat brains using monoclonal antibody 74-5H7 (Lemmon *et al.*, 1989). Both the anti-laminin Fabs used for control experiments and the experimental anti-L1 Fabs were produced according to the methods outlined by Mage (1980). The anti-laminin antibody only stains laminin located in the rat retinal basal lamina. When the anti-L1 Fab was used in culture at 200 $\mu\text{g}/\text{ml}$, it completely blocked axon outgrowth by chick retinal ganglion cells over a purified rat L1 substrate but not on a laminin substrate (unpublished observations). Goat anti-mouse IgG antibodies (Cappel) were also used in control experiments in this study. The procedures for preparation of polyclonal rabbit Ig and Fab's against rat NCAM along with their specificity have been previously described (Frelinger and Rutishauser, 1986). The anti-NCAM Fab fragments prevented rat brain vesicle aggregation in culture (unpublished observations). Fab's were then tested for their ability to penetrate the retinal neuroepithelium. Within 3 h of incubation, Fab's (500 $\mu\text{g}/\text{ml}$) could be detected with fluorescent secondary antibodies on the nerve fiber layer.

ACKNOWLEDGMENTS

We thank Cathy Doller and Denice Major for excellent technical assistance. A special thanks to both Mr. Weiss, for donating the Image 1 system, and Dr. Ross Payne, for his help with the Image 1 program. Supported by the National Institutes of Health (NIH Grants NS25713 to J.S., HD18369 and EY06107 to U.R., and EY05285 to V.L.), the Daniel Heumann Fund, and the Brumagin Memorial Fund.

REFERENCES

- Asou, H., Miura, M., Kobayashi, M., Uyemura, K., and Itoh, K. (1992). Cell adhesion molecule L1 guides cell migration in primary reaggregation cultures of mouse cerebellar cells. *Neurosci. Lett.* **144**: 221–224.

- Atashi, J. R., Klinz, S. G., Ingraham, C. A., Matten, W. T., Schachner, M., and Maness, P. F. (1992). Neural cell adhesion molecules modulate tyrosine phosphorylation of tubulin in nerve growth cone membranes. *Neuron* 8: 831–842.
- Barami, K., Kirschenbaum, B., Lemmon, V., and Goldman, S. A. (1994). N-cadherin and Ng-CAM/8D9 are serially involved in the migration of newly generated neurons into the adult songbird brain. *Neuron* 13: 567–582.
- Bastiani, M. J., Doe, C. Q., Helfand, S. L., and Goodman, C. S. (1985). Neuronal specificity and growth cone guidance in grasshopper and *Drosophila* embryos. *Trends Neurosci.* 8: 257–266.
- Bixby, J. L., and Jhabvala, P. (1990). Extracellular matrix molecules and cell adhesion molecules induce neurites through different mechanisms. *J. Cell Biol.* 111: 2725–2732.
- Brittis, P. A., and Silver, J. (1994). Exogenous glycosaminoglycans induce complete inversion of retinal ganglion cell bodies and their axons within the retinal neuroepithelium. *Proc. Natl. Acad. Sci. USA* 91: 7539–7542.
- Brittis, P. A., and Silver, J. (1995). Multiple factors govern intraretinal axon guidance: A time-lapse study. *Mol. Cell. Neurosci.* 6: 413–432.
- Brittis, P. A., Canning, D. R., and Silver, J. (1992). Chondroitin sulfate as a regulator of neuronal patterning in the retina. *Science* 255: 733–736.
- Brittis, P. A., Meiri, K., Dent, E., and Silver, J. (1995). The earliest patterns of neuronal differentiation and migration in the mammalian central nervous system. *J. Exp. Neurol.* 134: 1–12.
- Burden-Gulley, S. M., Payne, H. R., and Lemmon, V. (1995). Growth cones are actively influenced by substrate bound adhesion molecules. *J. Neurosci.* 15: 4370–4381.
- Burskirk, D. R., Thiery, J.-P., Rutishauser, U., and Edelman, G. M. (1980). Antibodies to a neural cell adhesion molecule disrupt histogenesis in cultured chick retinae. *Nature* 285: 488–489.
- Cervello, M., Lemmon, V., Landreth, G., and Rutishauser, U. (1991). Phosphorylation-dependent regulation of axon fasciculation. *Proc. Natl. Acad. Sci. USA* 88: 10548–10552.
- Chitnis, A. B., and Kuwada, J. Y. (1990). Axonogenesis in the brain of zebrafish embryos. *J. Neurosci.* 10: 1892–1905.
- Condic, M. L., Snow, D. M., and Letourneau, P. C. (1993). Regulation of laminin receptors by sensory neurons in response to chondroitin sulfate proteoglycan. *Soc. Neurosci. Abstr.* 19: 435.
- Cremer, H., Lange, R., Christoph, A., Plomann, M., Vopper, G., Roes, J., Brown, R., Baldwin, S., Kraemer, P., Scheff, S., et al. (1994). Inactivation of the N-CAM gene in mice results in size reduction of the olfactory bulb and deficits in spatial learning. *Nature* 367: 455–459.
- Cunningham, B. A., Hemperly, J. J., Murray, B. A., Prediger, E. A., Brackenbury, R., and Edelman, G. M. (1987). Neural cell adhesion molecule: Structure, immunoglobulin-like domains, cell surface modulation, and alternative RNA splicing. *Science* 236: 799–806.
- Doherty, P., and Walsh, F. S. (1989). Neurite guidance molecules. *Curr. Opin. Cell Biol.* 1: 1102–1106.
- Doherty, P., and Walsh, F. S. (1992). Cell adhesion molecules, second messengers and axonal growth. *Curr. Opin. Neurobiol.* 2: 595–601.
- Doherty, P., and Walsh, F. S. (1994). Signal transduction events underlying neurite outgrowth stimulated by cell adhesion molecules. *Curr. Opin. Neurobiol.* 4: 49–55.
- Drazba, J., and Lemmon, V. (1990). The role of cell adhesion molecules in neurite outgrowth on Muller cells. *Dev. Biol.* 138: 82–93.
- Easter, S. J., and Taylor, J. S. (1989). The development of the *Xenopus* retinofugal pathway: Optic fibers join a pre-existing tract. *Development* 107: 553–573.
- Frelinger, A. L., and Rutishauser, U. (1986). Topography of NCAM structure and functional determinants. II. Placement of monoclonal antibody epitopes. *J. Cell Biol.* 103: 1729–1737.
- Godement, P., Salaun, J., and Mason, C. A. (1990). Retinal axon pathfinding in the optic chiasm: Divergence of crossed and uncrossed fibers. *Neuron* 5: 173–186.
- Godement, P., Wang, L. C., and Mason, C. A. (1994). Retinal axon divergence in the optic chiasm: Dynamics of growth cone behavior at the midline. *J. Neurosci.* 14: 7024–7039.
- Goldberg, D. J., and Burmeister, D. W. (1986). Stages in axon formation: Observations of growth of *Aplysia* axons in culture using video-enhanced contrast-differential interference contrast microscopy. *J. Cell Biol.* 103: 1921–1931.
- Goldberg, S., and Coulombre, A. J. (1972). Topographical development of the ganglion cell fiber layer in the chick retina. A whole mount study. *J. Comp. Neurol.* 246: 507–518.
- Goodman, C. S. (1994). The likeness of being: Phylogenetically conserved molecular mechanisms of growth cone guidance. *Cell* 78: 353–356.
- Halfter, W. (1988). Aberrant optic axons in the retinal pigment epithelium during chick and quail visual pathway development. *J. Comp. Neurol.* 268: 161–170.
- Halfter, W., and Deiss, S. (1986). Axonal pathfinding in organ-cultured embryonic avian retinae. *Dev. Biol.* 114: 296–310.
- Halfter, W., and Fua, C. S. (1987). Immunohistochemical localization of laminin, neural cell adhesion molecule, collagen type IV and T-61 antigen in the embryonic retina of the Japanese quail by in vivo injection of antibodies. *Cell Tissue Res.* 249: 487–496.
- Halfter, W., Deiss, S., and Schwarz, U. (1985). The formation of the axonal pattern in the embryonic avian retina. *J. Comp. Neurol.* 232: 466–480.
- Hankin, M. H., and Lagenaur, C. F. (1994). Cell adhesion molecules in the early developing mouse retina: Retinal neurons show preferential outgrowth *in vitro* on L1 but not NCAM. *J. Neurobiol.* 25: 472–487.
- Jouet, M., Rosenthal, A., MacFarlane, J., and Kenrick, S. (1993). A missense mutation confirms the L1 defect in X-linked hydrocephalus (HSAS). *Nat. Genet.* 4: 331.
- Jouet, M., Rosenthal, A., Armstrong, G., MacFarlane, J., Stevenson, R., Paterson, J., Metzberg, A., Ionasescu, V., Temple, K., and Kenrick, S. (1994). X-linked spastic paraplegia (SPG1), MASA syndrome and X-linked hydrocephalus result from mutations in the L1 gene. *Nat. Genet.* 7: 402–407.
- Kapfhammer, J. P., and Raper, J. A. (1987). Collapse of growth cone structure on contact with specific neurites in culture. *J. Neurosci.* 7: 201–212.
- Kim, G. J., Shatz, C. J., and McConnell, S. K. (1991). Morphology of pioneer and follower growth cones in the developing cerebral cortex. *J. Neurobiol.* 22: 629–642.
- Kobayashi, H., Mizuki, T., Wada, A., and Izumi, F. (1992). Cell–cell contact modulates expression of cell adhesion molecule L1 in PC12 cells. *Neuroscience* 49: 437–441.
- Krayanek, S., and Goldberg, S. (1981). Oriented extracellular channels and axonal guidance in the embryonic chick retina. *Dev. Biol.* 84: 41–50.
- Lagenaur, C., and Lemmon, V. (1987). An L1-like molecule, the 8D9 antigen, is a potent substrate for neurite extension. *Proc. Natl. Acad. Sci. USA* 84: 7753–7757.
- Lander, A. D. (1987). Molecules that make axons grow. *Mol. Neurobiol.* 1: 213–245.
- Landmesser, L., Dahm, L., Schultz, K., and Rutishauser, U. (1988). Distinct roles for adhesion molecules during innervation of embryonic chick muscle. *Dev. Biol.* 130: 645–670.
- Lemmon, V., and McLoon, S. C. (1986). The appearance of an L1-like molecule in the chick primary visual pathway. *J. Neurosci.* 6: 2987–2994.
- Lemmon, V., Farr, K. L., and Lagenaur, C. (1989). L1-mediated axon outgrowth occurs via a homophilic binding mechanism. *Neuron* 2: 1597–1603.

- Lemmon, V., Burden, S. M., Payne, H. R., Elmslie, G. J., and Hlavin, M. L. (1992). Neurite growth on different substrates: Permissive versus instructive influences and the role of adhesive strength. *J. Neurosci.* **12**: 818–826.
- Lindner, J., Rathjen, F. G., and Schachner, M. (1983). L1 mono- and polyclonal antibodies modify cell migration in early postnatal mouse cerebellum. *Nature* **305**: 427–430.
- Mage, M. G. (1980). Preparation of Fab fragments from IgGs of different animal species. *Methods Enzymol.* **70**: 142–150.
- Mann, I. (1969). *The Development of the Human Eye*. Grune & Stratton, New York.
- Martini, R., Xin, Y., and Schachner, M. (1994). Restricted localization of L1 and NCAM at sites of contact between Schwann cells and neurites in culture. *Glia* **10**: 70–74.
- Miura, M., Asou, H., Kobayashi, M., and Uyemura, K. (1992). Functional expression of a full-length cDNA coding for rat neural cell adhesion molecule L1 mediates homophilic intercellular adhesion and migration of cerebellar neurons. *J. Biol. Chem.* **267**: 10752–10758.
- Moos, M., Tacke, R., Scherer, H., Teplow, D., Fruh, K., and Schachner, M. (1988). Neural adhesion molecule L1 as a member of the immunoglobulin superfamily with binding domains similar to fibronectin. *Nature* **334**: 701–703.
- Overton, J. (1979). Differential response of embryonic cells to culture on tissue matrices. *Tissue Cell* **11**: 89–98.
- Payne, H. R., Burden, S. M., and Lemmon, V. (1992). Modulation of growth cone morphology by substrate-bound adhesion molecules. *Cell Motil. Cytoskeleton* **21**: 65–73.
- Pollerberg, G. E., Schachner, M., and Davoust, J. (1986). Differentiation state-dependent surface mobilities of two forms of the neural cell adhesion molecule. *Nature* **324**: 462–465.
- Rager, G., and von Oeynhaus, B. (1979). Ingrowth and ramification of retinal fibers in the developing optic tectum of the chick embryo. *Exp. Brain Res.* **35**: 213–227.
- Raper, J. A., Bastiani, M., and Goodman, C. S. (1983). Pathfinding by neuronal growth cones in grasshopper embryos. II. Selective fasciculation onto specific axonal pathways. *J. Neurosci.* **3**: 31–41.
- Redies, C., and Takeichi, M. (1993). N- and R-cadherin expression in the optic nerve of the chicken embryo. *Glia* **8**: 161–171.
- Reichardt, L. F., Bixby, J. L., Hall, D. E., Ignatius, M. J., Neugebauer, K. M., and Tomaselli, K. J. (1989). Integrins and cell adhesion molecules: Neuronal receptors that regulate axon growth on extracellular matrices and cell surfaces. *Dev. Neurosci.* **11**: 332–347.
- Rosenthal, A., Jouet, M., and Kenwrick, S. (1992). Aberrant splicing of neural cell adhesion molecule L1 messenger RNA in a family with X-linked hydrocephalus. *Nat. Genet.* **2**: 107–112.
- Rutishauser, U., Watanabe, M., Silver, J., Troy, F. A., and Vimir, E. R. (1985). Specific alteration of NCAM-mediated cell adhesion by an endoneuraminidase. *J. Cell Biol.* **101**: 1842–1849.
- Schachner, M., and Maness, P. F. (1992). Neural cell adhesion molecules modulate tyrosine phosphorylation of tubulin in nerve growth cone membranes. *Neuron* **8**: 831–842.
- Schlosshauer, B., and Duting, D. (1991). Intraretinal pathfinding of ganglion cell axons is perturbed by a monoclonal antibody specific for a G4/Ng-CAM-like cell adhesion molecule. *Dev. Brain Res.* **63**: 181–190.
- Schuch, U., Lohse, M. J., and Schachner, M. (1989). Neural cell adhesion molecules influence second messenger systems. *Neuron* **3**: 13–20.
- Silver, J., and Rutishauser, U. (1984). Guidance of optic axons in vivo by a preformed adhesive pathway on neuroepithelial endfeet. *Dev. Biol.* **106**: 485–499.
- Silver, J., and Sidman, R. L. (1980). A mechanism for the guidance and topographic patterning of retinal ganglion cell axons. *J. Comp. Neurol.* **189**: 101–111.
- Smith, G. M., Rutishauser, U., Silver, J., and Miller, R. H. (1990). Maturation of astrocytes in vitro alters the extent and molecular basis of neurite outgrowth. *Dev. Biol.* **138**: 377–390.
- Smith, C. L. (1994). Cytoskeletal movements and substrate interactions during initiation of neurite outgrowth by sympathetic neurons in vitro. *J. Neurosci.* **14**: 384–398.
- Snow, D. M., and Letourneau, P. C. (1992). Neurite outgrowth on a step gradient of chondroitin sulfate proteoglycan (CS-PG). *J. Neurobiol.* **23**: 322–336.
- Snow, D. M., Watanabe, M., Letourneau, P. C., and Silver, J. (1991). A chondroitin sulfate proteoglycan may influence the direction of retinal ganglion cell outgrowth. *Development* **113**: 1473–1485.
- Sretavan, D. W., Feng, L., Pure, E., and Reichardt, L. F. (1994). Embryonic neurons at the developing optic chiasm express L1 and CD44 cell surface molecules with opposing effects on retinal axon growth. *Neuron* **12**: 957–975.
- Stallcup, W. B., and Beasley, L. (1985). Involvement of the nerve growth factor-inducible large external glycoprotein (NILE) in neurite fasciculation in primary cultures of rat brain. *Proc. Natl. Acad. Sci. USA* **82**: 1276–1280.
- Suburo, A., Carri, N., and Adler, R. (1979). The environment of axonal migration in the developing chick retina: A scanning electron microscopic study. *J. Comp. Neurol.* **184**: 519–536.
- Thanos, S., and Bonhoeffer, F. (1987). Axonal arborization in the developing chick retinotectal system. *J. Comp. Neurol.* **261**: 155–164.
- Tomasiewicz, H., Ono, K., Yee, D., Thompson, C., Goridis, C., Rutishauser, U., and Magnuson, T. (1993). Genetic deletion of a neural cell adhesion molecule variant (N-CAM-180) produces distinct defects in the central nervous system. *Neuron* **11**: 1163–1174.
- Tosney, K. W., and Oakley, R. A. (1990). The perinotochordal mesenchyme acts as a barrier to axon advance in the chick embryo: Implications for a general mechanism of axonal guidance. *Exp. Neurol.* **109**: 75–89.
- Van Camp, G., Vits, L., Coucke, P., Lyonnet, S., Schrandt-Stumpel, C., Darby, J., Holden, J., Munnich, A., and Willems, P. J. (1993). A duplication in the L1CAM gene associated with X-linked hydrocephalus. *Nat. Genet.* **4**: 421–425.
- Vits, L., Van Camp, G., Coucke, P., Franssen, E., DeBoufle, K., Reyniers, E., Korn, B., Poustka, A., Wilson, G., Schrandt-Stumpel, C., Winter, R. M., Schwartz, C. E., and Willems, P. J. (1994). MASA syndrome is due to mutations in the neural cell adhesion gene L1CAM. *Nat. Genet.* **7**: 408–413.
- Vonbohlen, F., Halbach, Taylor, J., and Schachner, M. (1992). Cell type-specific effects of the neural adhesion molecules L1 and N-CAM on diverse second messenger systems. *Eur. J. Neurosci.* **4**: 896–909.
- Williams, E. J., Furness, J., Walsh, F. S., and Doherty, P. (1994). Activation of the FGF receptor underlies neurite outgrowth stimulated by L1, NCAM and N-cadherin. *Neuron* **13**: 583–594.
- Williams, R. W., Borodkin, M., and Rakic, P. (1991). Growth cone distribution patterns in the optic nerve of fetal monkeys: Implications for mechanisms of axon guidance. *J. Neurosci.* **11**: 1081–1094.
- Wilson, S. W., Ross, L. S., Parrett, T., and Easter, S. J. (1990). The development of a simple scaffold of axon tracts in the brain of the embryonic zebrafish, *Brachydanio rerio*. *Development* **108**: 121–145.